

Nanoscale

Accepted Manuscript



This is an *Accepted Manuscript*, which has been through the Royal Society of Chemistry peer review process and has been accepted for publication.

Accepted Manuscripts are published online shortly after acceptance, before technical editing, formatting and proof reading. Using this free service, authors can make their results available to the community, in citable form, before we publish the edited article. We will replace this *Accepted Manuscript* with the edited and formatted *Advance Article* as soon as it is available.

You can find more information about *Accepted Manuscripts* in the [Information for Authors](#).

Please note that technical editing may introduce minor changes to the text and/or graphics, which may alter content. The journal's standard [Terms & Conditions](#) and the [Ethical guidelines](#) still apply. In no event shall the Royal Society of Chemistry be held responsible for any errors or omissions in this *Accepted Manuscript* or any consequences arising from the use of any information it contains.

ARTICLE

Atomic Layer Deposition of MoS₂ film

Cite this: DOI: 10.1039/x0xx00000x Lee Kheng Tan,^{‡ab} Bo Liu,^{‡c} Jing Hua Teng,^b Shifeng Guo,^b Hong Yee Low,^d and Kian Ping Loh^{*a}

Received 00th January 2012,
Accepted 00th January 2012

DOI: 10.1039/x0xx00000x

www.rsc.org/

Mono- to multilayer thick MoS₂ film has been grown by atomic layer deposition (ALD) technique at 300 °C on sapphire wafer. ALD provides precise control of MoS₂ film thickness due to pulsed introduction of the reactants and self-limiting reactions of MoCl₅ and H₂S. A post-deposition annealing of the ALD-deposited monolayer film improves the crystallinity of the film, which is evident from the presence of triangle-shaped crystals that exhibit strong photoluminescence in the visible range.

1. Introduction

Two dimensional transition-metal dichalcogenides (TMDCs) are the “semiconductor” analogues of graphene. Due to its 2D confinement, TMDCs show unique electronic and optical properties which can be applied in light harvesting or photochemical devices.¹⁻³ Some unique properties of the monolayer film compared to the bulk crystal include indirect-to-direct band transitions⁴⁻⁶ and valley polarization.^{7,8} Among various TMDCs, molybdenum disulphide (MoS₂) has been intensively studied because of its excellent optical⁹⁻¹¹, electrochemical¹²⁻¹⁴ and electrical properties.^{1,15-17} There are many approaches to grow this atomically thin film. Mechanical exfoliation¹⁸⁻²⁰ has been the workhorse to prepare high quality monolayer MoS₂ flakes, but it suffers from small sample size and scalability. Synthetic methods such as liquid exfoliation^{9,21,22}, chemical vapour deposition (CVD)^{23,24}, hydrothermal²⁵ and electrochemical¹² methods are limited by the small surface areas of the samples, lack of control of film thickness and produce generally poor crystalline quality films. Precise growth of atomic layered MoS₂ films over a large area remains a challenge.

Atomic layer deposition (ALD)^{26,27} affords precise film thickness control because it involves sequential and repeated exposure of precursor vapours that undergo self-limiting reactions on the substrate surface. ALD also offers the benefit of wafer scale fabrication of various inorganic films, including oxides, nitrides, metals and chalcogenides.²⁸⁻³⁰

In this work, we report the ALD of MoS₂ film on sapphire substrate. MoS₂ films are prepared by alternating exposure of molybdenum (V) chloride (MoCl₅) and hydrogen disulphide (H₂S) vapours (see experimental section for details). Due to the self-limiting reactions of the vapours, the number of MoS₂ film layers can be precisely controlled by the number of deposition cycles. As our ALD system only allows an upper temperature limit of 300 °C on the substrate, we performed a post-annealing at 800 °C to

improve film crystallinity; the as-deposited film on sapphire can be restructured to produce faceted triangular crystals.

2. Experimental section

2.1 Growth of ALD MoS₂ film

c-plane single crystal sapphire (Al₂O₃ > 99.99%) with <0001> orientation, 2-inch diameter, 0.5 mm thick and single side polished was cleaned successively in acetone and isopropanol using an ultrasonic bath. MoS₂ film was deposited in a home-built ALD setup. The sapphire substrate was alternately exposed to vapours of anhydrous MoCl₅ (Strem, 99.6%) and H₂S (NOX, 3.5%, balance N₂) at a base pressure of 1 × 10⁻³ torr at 300 °C. The temperature of MoCl₅ source was kept at 120 °C to generate sufficient vapour pressure, and this is carried in N₂ at a flow rate of 20 sccm. The dosing conditions for the MoCl₅ precursor are: a 5 s exposure time, 5 s dwelling time and 30 s N₂ purging time. H₂S precursor have a 0.1 s exposure time, 5 s dwelling time and 20 s N₂ purging time.

2.2 Annealing of ALD MoS₂ film.

MoS₂ film was annealed under saturated sulfur vapour in a tube furnace (MTI OTF-1200X) at 800 °C, with a ramping rate of 50 K/min and a dwelling for 30 mins. The annealing was performed under saturated sulfur vapour to prevent any oxidation or evaporation of the as-deposited film.

3. Results and discussion

Fig. 1 depicts the schematic diagram of a complete one growth cycle of ALD of MoS₂ on sapphire substrate. One growth cycle consists of six main steps: 1) 5 s exposure to MoCl₅ 2) 5 s dwelling 3) 30 s N₂ purge 4) 0.1 s exposure to H₂S 5) 5 s dwelling 6) 20 s N₂ purge. In the ALD process, nucleation is an

important step.³¹ Nucleation is difficult on a lattice-mismatched substrate. Thus, instead of using continuous flow mode, we use a quasi-static mode³² in a viscous flow ALD chamber. The quasi-static mode has an additional dwelling step so that precursors have ample time to react with substrate surface. This will increase nucleation rate (faster formation of a continuous layer) and promotes surface reactions. The cycle is repeated until the desired film thickness is reached. As shown in Fig. 1, the MoS₂ film deposited on a 2 inch size sapphire (001) substrate changes to a darker shade from 10 to 50 ALD cycles.

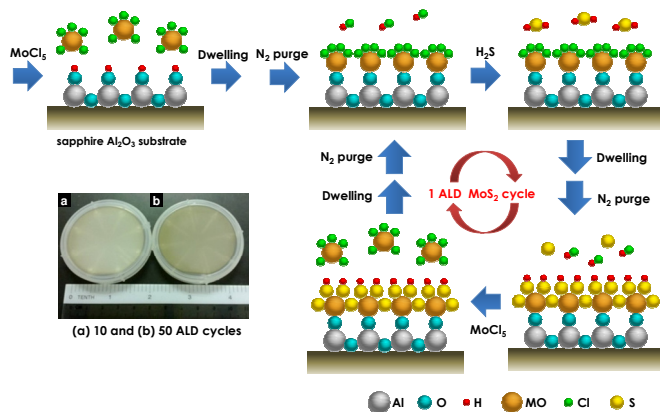


Fig. 1 Schematic illustration of one growth cycle of ALD MoS₂ film. The photograph shows (a) 10 and (b) 50 cycles of ALD MoS₂ film grown on 2-inch sapphire (001) substrate.

To perform TEM, the as-grown MoS₂ films were exfoliated from the substrate and suspended on a lacey carbon TEM grid. Fig. 2a shows planar view of the lattice planes in mono- and multilayered MoS₂ film grown by ALD. The typical atomic spacing is indicated in Fig. 2b. The Fast Fourier transformation (FFT) pattern (inset) shows hexagonal lattice structure with d-spacing of 0.274 nm and 0.162 nm for lattice planes (100) and (110) respectively.²⁴ The grain boundaries between two MoS₂ domains can be easily seen in this TEM image, indicated by dotted white lines. Cross-sectional view of

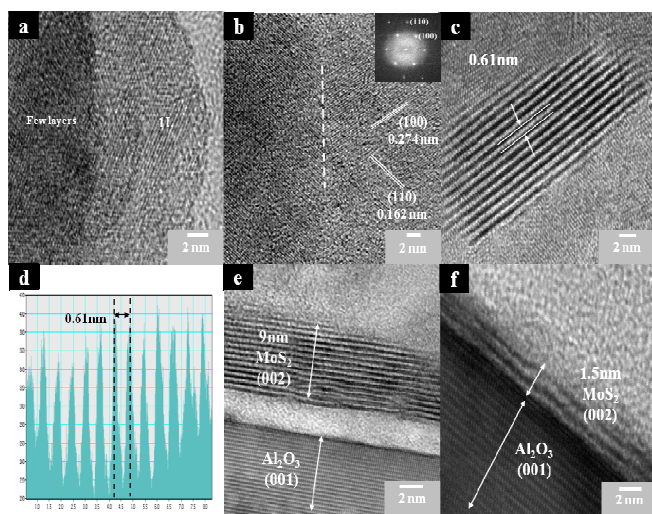


Fig. 2 (a) TEM image of mono- and multilayered ALD MoS₂ film exfoliated from (001) sapphire substrate and suspended on TEM grid for imaging. (b) TEM image of MoS₂ film reveals crystalline film grown by ALD. The inset FFT pattern confirms the hexagonal lattice structure. (c) Lattice spacing from cross-sectional TEM view (d) Line profile shows the layer spacing in (c). Cross-sectional TEM view of (e) 50 cycles ALD MoS₂ film. (f) 10 cycles ALD MoS₂ film. The substrate is sapphire.

MoS₂ film in Fig. 2c and its intensity profile in Fig. 2d clearly show the inter-planar spacing of 0.610 nm for the (002) planes. The TEM images in Fig. 2e and 2f provide evidence of the precise thickness control of ALD technique by simply controlling the number of ALD cycles. A gap between the MoS₂ film and sapphire substrate is observed at Fig. 2e as the film was delaminated from the substrate during sample preparation for TEM. The film thickness of ~9 nm (Fig. 2e) and ~1.5 nm (Fig. 2f) corresponds to 50 and 10 ALD cycles respectively.

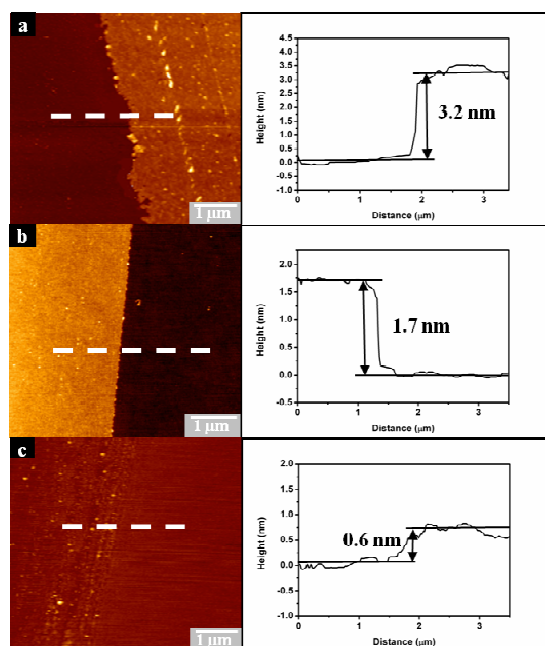


Fig. 3 AFM images and height profiles of (a) 20 (b) 10 (c) 5 cycles of as-grown ALD MoS₂ film on sapphire substrate.

Fig. 3a to 3c shows the AFM images and height profiles of 20, 10 and 5 cycles respectively of as-grown ALD MoS₂ films on sapphire substrate. The film thicknesses are ~3.2 nm, ~1.7 nm and ~0.6 nm, respectively. As reported previously, the thickness of one monolayer of MoS₂ film ranges between 0.6 to 1.2 nm, depending on the preparation method and the surface interactions between MoS₂ flake and substrate.^{9,24,33} We observed that at least 10 ALD cycles are required for the formation of a complete MoS₂ monolayer film, which has a film thickness of ~1.7 nm. The AFM images in Fig. S1 (ESI[†]) compares the changes in morphology for 5 and 10 ALD cycles within an area of 5 × 5 μm². 5 ALD cycles result in early-stage island growth and incomplete coverage on the substrate. 10 ALD cycles produce a continuous, ~1.7 nm thick monolayer film, as shown by the TEM image in Fig. S2 (ESI[†]). The MoS₂ film grown on sapphire substrate is subsequently transferred onto Si substrate

for photoluminescence (PL) measurements, as shown in Fig. S3 (ESI†). The relationship between the number of ALD cycles and film thickness, as measured by both TEM imaging and AFM height profiles, is shown in Fig. S4 (ESI†).

To improve the crystallinity of the film, the as-deposited film was subjected to a post-annealing step at 500 °C, 700 °C or 800 °C in sulfur vapour. Fig. 4a shows optical absorption spectra of 30 ALD cycles of MoS₂ film on sapphire and the inset plots the differential absorption spectra. The as-grown MoS₂ thin film on sapphire does not show any excitonic features in the optical absorption. This could be due to the poor crystallinity of the as-grown film at 300 °C. After annealing between 700-800 °C, excitonic peaks A (~ 1.85 eV) and B (~ 2.00 eV) appear.^{34,35} This suggests that high temperature annealing is able to reconstruct the as-grown film and improves its crystallinity.

Steady-state PL spectra of MoS₂ film deposited by 10, 20 and 30 ALD cycles, before and after 800 °C annealing, is shown in Fig. 4b. The sharp twin peak at 694 nm is due to the sapphire substrate. To uncouple the influence of the sapphire substrate, we transferred the film onto SiO₂ (Fig. S3 ESI†). No excitonic peak was observed on as-grown ALD films at first. After annealing at 800 °C, the monolayer film grown by 10 ALD cycles shows a distinct peak at 665 nm (1.86 eV) and a weak peak at 630 nm. With increasing thickness of the MoS₂ film, the PL intensities weaken, which is explained by the change in optical band gap from direct to indirect.⁴⁻⁶ Fluctuation in the excitonic peak position is attributed to the unintentional doping by the substrate or environment.^{36,37}

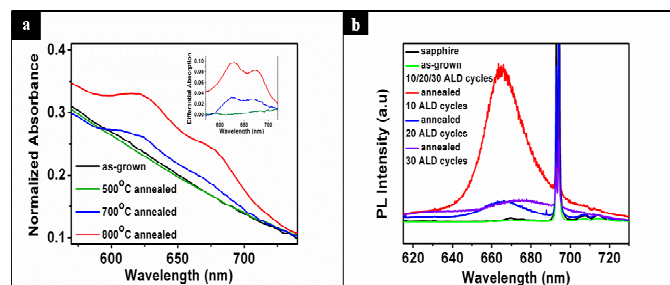


Fig. 4 (a) Optical absorption (b) Photoluminescence spectra for ALD-deposited, as-grown or annealed MoS₂ films.

As discussed, MoS₂ film which is grown by at least 10 ALD cycles, and which has been subjected to an annealing temperature of 800 °C, is found to possess good crystalline quality. Fig. 5a shows SEM image of one such film where triangular MoS₂ crystals are observed on the sapphire substrate. Fig. 5b, reveal that these triangle flakes are typically ~2 μm in width. Thermal re-structuring reduces the thickness of the flakes to ~0.8 nm, as compared to ~1.7 nm before annealing. For 20 ALD cycles, a much thicker, continuous film is formed. The height profile of the 20 ALD cycles film after annealing was measured and the thickness was found to decrease from ~3.2 nm to ~1.3 nm after the annealing process as shown in Fig. S5 (ESI†).

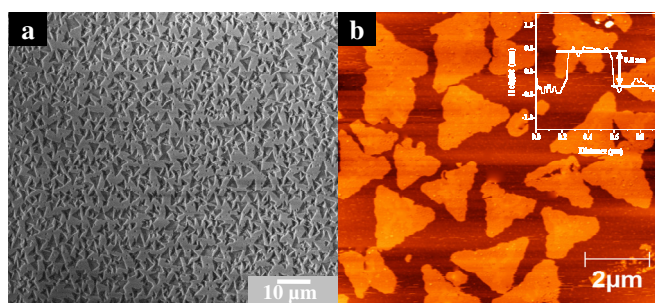


Fig 5 (a) SEM and (b) AFM images of monolayer 800 °C-annealed ALD MoS₂ film. The inset shows the height profile of the triangular flakes.

The improvement in MoS₂ film crystallinity after annealing is also as evident from the XRD and Raman spectrum. As shown in Fig. 6a, diffraction peak intensities of 50 ALD cycles film increase by four times after annealing compared to as-grown film. The characteristic sharp MoS₂ (002) diffraction peak at 2θ = 14.5 is clearly evident in the XRD spectra. This lattice plane corresponds to the interplanar spacing of 0.610 nm in TEM image Fig. 2c.

Both A_{1g} and E_{2g} vibrational modes, which are associated with out-of-plane vibration of sulfur atoms and in-plane vibration of Mo and S atoms, respectively³⁸⁻⁴⁰ can be observed clearly in the Raman spectrum (Fig. 6b). The Raman peaks intensities increase with ALD cycles for both as-grown and annealed films. In addition, the Raman peaks clearly sharpen after the annealing process and the frequency difference (Δk) between A_{1g} and E_{2g} modes reduces, which is indicative of improved crystallinity in the films. Previously, Δk has been used as a parameter to predict the thickness of the MoS₂ layers. However, ALD monolayer film produced by 10 ALD cycles shows a relatively large Δk of 26 cm⁻¹ (after annealing) compared to 19.4 cm⁻¹ of the exfoliated MoS₂ flakes. Due to rotational stacking disorder,⁹ direct determination of film thickness from Δk is not possible for ALD grown MoS₂ film.

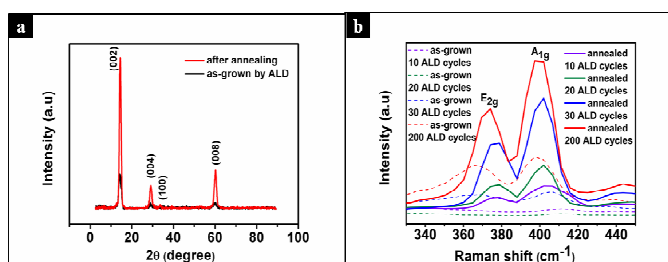


Fig 6 (a) XRD and (b) Raman spectra for as-grown and 800°C-annealed ALD MoS₂ films.

The bonding characteristics and stoichiometry of as-grown and annealed MoS₂ films is studied by X-ray photoelectron spectroscopy (XPS). Fig. 7 shows the characteristic Mo 3d doublet peaks and S 2s peaks with binding energies (BE) around 232.6 eV, 229.4 eV and 226.9 eV, respectively. The as-grown film reveals a partially resolved S 2p doublet at 163.4 eV and 162.2 eV while this doublet is seen to be sharper after annealing. These observations are consistent with previous report.⁹ The calculated stoichiometric ratio is 1.97

(S/Mo) before annealing and 2.03 after annealing in sulfur, which suggests that the as-grown film may be slightly sulphur deficient.

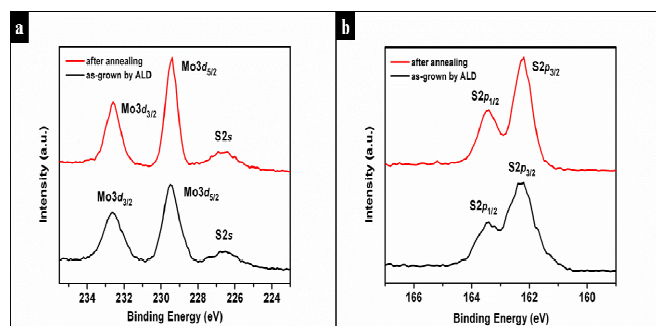


Fig 7 XPS spectra of (a) Mo 3d, S 2s and (b) S 2p core level peaks for as-grown and 800°C-annealed ALD MoS₂ film.

The instrumental restriction in our ALD deposition system precludes deposition at substrate temperatures above 300 °C. It is expected that if the deposition is carried out at elevated temperatures, but not exceeding the window for ALD process, the quality of the film should be significantly improved.

4. Conclusions

In summary, atomically thin, highly crystalline MoS₂ film can be prepared by ALD deposition on sapphire substrate. Due to the precise film thickness control by ALD technique, wafer-scale mono- and multilayer MoS₂ films can be readily prepared. Post annealing of the as-deposited MoS₂ film further improves its crystallinity, as evidenced by the strong PL emission from the monolayer film after annealing.

Acknowledgements

We thank the Institute of Materials Research and Engineering under the Agency for Science, Technology and Research (A*STAR) Singapore as well as Singapore-Berkeley Research Initiative for Sustainable Energy (SinBeRISE) CREATE Program for the financial support. We are grateful to Ms Tan Hui Ru for her assistance in HRTEM, Mr Lim Poh Chong for his assistance in XRD, Ms June Ong for her assistance in XPS and Dr Liu Hong Fei for his advice.

Notes and references

^a Department of Chemistry and Graphene Research Centre
National University of Singapore

3 Science Drive 3
Singapore 117543
chmlohkp@nus.edu.sg

^b A*STAR, Institute of Materials Research and Engineering,
3 Research Link
Singapore 117602

^c Department of Physics and Graphene Research Centre
National University of Singapore
2 Science Drive 3
Singapore 117551

^d Singapore University of Technology and Design
20 Dover Dr

Singapore 138682

‡These authors contributed equally.

†Electronic Supplementary Information (ESI) available: See
DOI: 10.1039/b000000x/

References

1. B. Radisavljevic, A. Radenovic, J. Brivio, V. Giacometti, and A. Kis, *Nat.Nanotechnol.*, 2011, **6**, 147.
2. H. R. Gutierrez, N. Perea-Lopez, A. L. Elias, A. Berkdemir, B. Wang, R. Lv, F. Lopez-Urias, V. H. Crespi, H. Terrones, and M. Terrones, *Nano Lett.*, 2013, **13**, 3447.
3. W. S. Yun, S. W. Han, S. C. Hong, I. G. Kim, and J. D. Lee, *Phys.Rev.B: Condens.Matter Mater.Phys.*, 2012, **85**, 033305/1.
4. T. Li and G. Galli, *J.Phys.Chem.C*, 2007, **111**, 16192.
5. K. F. Mak, C. Lee, J. Hone, J. Shan, and T. F. Heinz, *Phys.Rev.Lett.*, 2010, **105**, 136805/1.
6. J. K. Ellis, M. J. Lucero, and G. E. Scuseria, *Appl.Phys.Lett.*, 2011, **99**, 261908/1.
7. H. Zeng, J. Dai, W. Yao, D. Xiao, and X. Cui, *Nat.Nanotechnol.*, 2012, **7**, 490.
8. K. F. Mak, K. He, J. Shan, and T. F. Heinz, *Nat.Nanotechnol.*, 2012, **7**, 494.
9. G. Eda, H. Yamaguchi, D. Voiry, T. Fujita, M. Chen, and M. Chhowalla, *Nano Lett.*, 2011, **11**, 5111.
10. T. Korn, S. Heydrich, M. Hirmer, J. Schmutzler, and C. Schueller, *Appl.Phys.Lett.*, 2011, **99**, 102109/1.
11. A. Splendiani, L. Sun, Y. Zhang, T. Li, J. Kim, C. Y. Chim, G. Galli, and F. Wang, *Nano Lett.*, 2010, **10**, 1271.
12. J. D. Benck, Z. Chen, L. Y. Kuritzky, A. J. Forman, and T. F. Jaramillo, *ACS Catal.*, 2012, **2**, 1916.
13. D. Merki, S. Fierro, H. Vrubel, and X. Hu, *Chem.Sci.*, 2011, **2**, 1262.
14. D. Voiry, M. Salehi, R. Silva, T. Fujita, M. Chen, T. Asefa, V. B. Shenoy, G. Eda, and M. Chhowalla, *Nano Lett.*, 2013, **13**, 6222.
15. B. Radisavljevic and A. Kis, *Nat.Mater.*, 2013, **12**, 815.
16. Q. H. Wang, K. Kalantar-Zadeh, A. Kis, J. N. Coleman, and M. S. Strano, *Nat.Nanotechnol.*, 2012, **7**, 699.
17. W. Zhang, C. P. Chuu, J. K. Huang, C. H. Chen, M. L. Tsai, Y. H. Chang, C. T. Liang, Y. Z. Chen, Y. L. Chueh, J. H. He, M. Y. Chou, and L. J. Li, *Sci.Rep.*, 2014, **4**.
18. M. Chhowalla, H. S. Shin, G. Eda, L. J. Li, K. P. Loh, and H. Zhang, *Nat Chem*, 2013, **5**, 263.
19. B. K. Miremadi and S. R. Morrison, *J.Catal.*, 1987, **103**, 334.
20. P. Joensen, R. F. Frindt, and S. R. Morrison, *Mater.Res.Bull.*, 1986, **21**, 457.
21. J. N. Coleman, M. Lotya, A. O'Neill, S. D. Bergin, P. J. King, U. Khan, K. Young, A. Gaucher, S. De, R. J. Smith, I. V. Shvets, S. K. Arora, G. Stanton, H. Y. Kim, K. Lee, G. T. Kim, G. S. Duesberg, T. Hallam, J. J. Boland, J. J. Wang, J. F. Donegan, J. C. Grunlan, G. Moriarty, A. Shmeliov, R. J. Nicholls, J. M. Perkins, E. M. Grievson, K. Theuwissen, D. W. McComb, P. D. Nellist, and V. Nicolosi, *Science (Washington, DC, U.S.)*, 2011, **331**, 568.

22. J. Zheng, H. Zhang, S. Dong, Y. Liu, C. T. Nai, H. S. Shin, H. Y. Jeong, B. Liu, and K. P. Loh, *Nat. Commun.*, 2014, **5**, 3995/1.
23. M. R. Laskar, L. Ma, S. Kannappan, P. S. Park, S. Krishnamoorthy, D. N. Nath, W. Lu, Y. Wu, and S. Rajan, *Appl. Phys. Lett.*, 2013, **102**, 252108/1.
24. Y. H. Lee, X. Q. Zhang, W. Zhang, M. T. Chang, C. T. Lin, K. D. Chang, Y. C. Yu, J. T.-W. Wang, C. S. Chang, L. J. Li, and T. W. Lin, *Adv Mater*, 2012, **24**, 2320.
25. Y. Peng, Z. Meng, C. Zhong, J. Lu, W. Yu, Y. Jia, and Y. Qian, *Chem. Lett.*, 2001772.
26. S. M. George, *Chem. Rev. (Washington, DC, U.S.)*, 2010, **110**, 111.
27. G. N. Parsons, J. W. Elam, S. M. George, S. Haukka, H. Jeon, W. M. M. Kessels, M. Leskela, P. Poodt, M. Ritala, and S. M. Rossnagel, *J. Vac. Sci. Technol., A*, 2013, **31**, 050818/1.
28. J. E. Crowell, *J. Vac. Sci. Technol., A*, 2003, **21**, S88.
29. V. Miikkulainen, M. Leskela, M. Ritala, and R. L. Puurunen, *J. Appl. Phys. (Melville, NY, U.S.)*, 2013, **113**, 021301/1.
30. J. S. Ponraj, G. Attolini, and M. Bosi, *Crit. Rev. Solid State Mater. Sci.*, 2013, **38**, 203.
31. Pinna, N., M. Knez, and Editors, *Atomic Layer Deposition of Nanostructured Materials*. 2012: Wiley-VCH Verlag GmbH & Co. KGaA. 435.
32. Elam, J.W., et al., *Chem. Mater.*, 2003, **15**(18), 3507-3517
33. N. Liu, P. Kim, J. H. Kim, J. H. Ye, S. Kim, and C. J. Lee, *ACS Nano*, 2014, Article ASAP.
34. R. Coehoorn, C. Haas, J. Dijkstra, C. J. F. Flipse, R. A. de Groot, and A. Wold, *Phys. Rev. B*, 1987, **35**, 6195.
35. R. Coehoorn, C. Haas, and R. A. de Groot, *Phys. Rev. B*, 1987, **35**, 6203.
36. K. F. Mak, K. He, C. Lee, G. H. Lee, J. Hone, T. F. Heinz, and J. Shan, *Nat. Mater.*, 2013, **12**, 207.
37. S. Mouri, Y. Miyauchi, and K. Matsuda, *Nano Lett.*, 2013, **13**, 5944.
38. C. Lee, H. Yan, L. E. Brus, T. F. Heinz, J. Hone, and S. Ryu, *ACS Nano*, 2010, **4**, 2695.
39. B. S.-L. Li, H. Miyazaki, H. Song, H. Kuramochi, S. Nakaharai, and K. Tsukagoshi, *ACS Nano*, 2012, **6**, 7381.
40. H. Li, Q. Zhang, C. C. R. Yap, B. K. Tay, T. H. T. Edwin, A. Olivier, and D. Baillargeat, *Adv. Funct. Mater.*, 2012, **22**, 1385.